

# m6A and NuRD complexes regulate monocytic differentiation and resistance to BCL2/BCL2L1 inhibitors in acute myeloid leukemia

Jackson Brim-Edwards,<sup>1,2</sup> Karen Morris,<sup>1,2</sup> Quinlan Morrow,<sup>1,2</sup> Stephen E. Kurtz,<sup>2,3</sup> Daniel Bottomly,<sup>2</sup> Shannon K. McWeeney,<sup>2,4</sup> Cristina E. Tognon,<sup>2,3</sup> Tamilla Nechiporuk,<sup>1,2</sup> Kevin Watanabe-Smith<sup>2,3#</sup> and Jeffrey W. Tyner<sup>1,2,5#</sup>

<sup>1</sup>Department of Cell, Developmental & Cancer Biology; <sup>2</sup>Knight Cancer Institute; <sup>3</sup>Division of Oncological Sciences, Knight Cancer Institute; <sup>4</sup>Division of Bioinformatics and Computational Biology, Department of Medical Informatics and Clinical Epidemiology and <sup>5</sup>Division of Hematology and Medical Oncology, Oregon Health & Science University, Portland, OR, USA

*#KW-S and JWT contributed equally as senior authors.*

**Correspondence:** J.W. Tyner  
[tynerj@ohsu.edu](mailto:tynerj@ohsu.edu)

**Received:** April 9, 2025.

**Accepted:** October 3, 2025.

**Early view:** October 16, 2025.

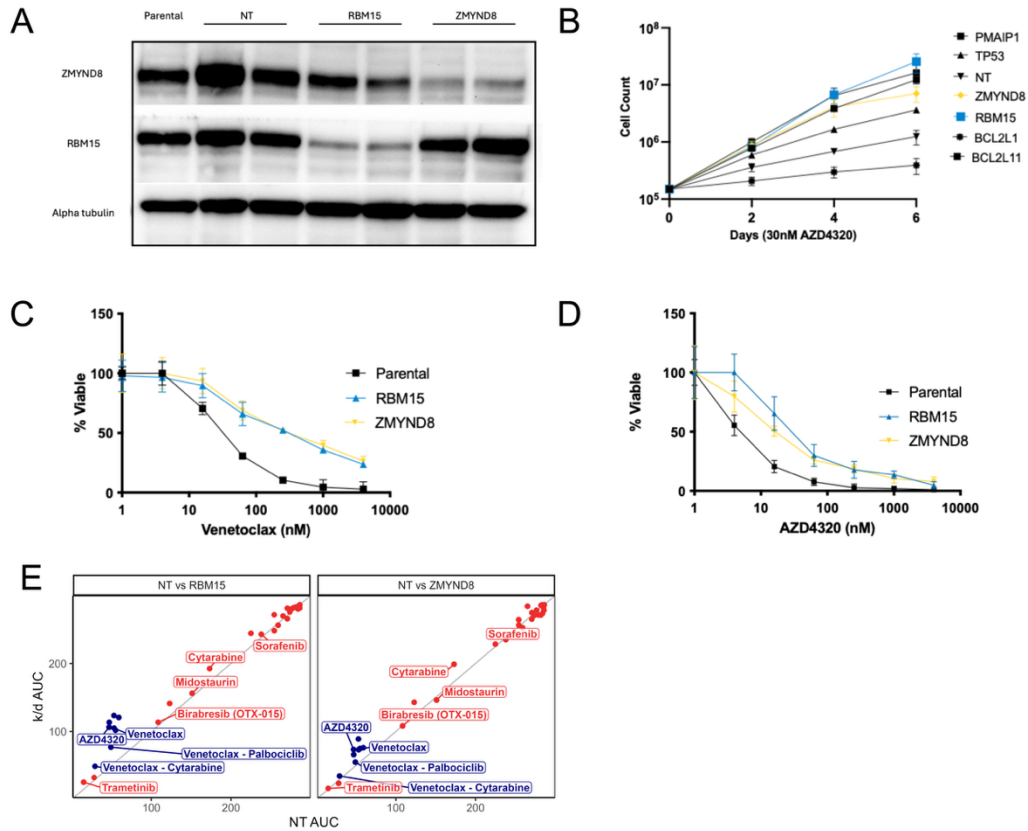
<https://doi.org/10.3324/haematol.2025.287972>

©2026 Ferrata Storti Foundation

Published under a CC BY-NC license

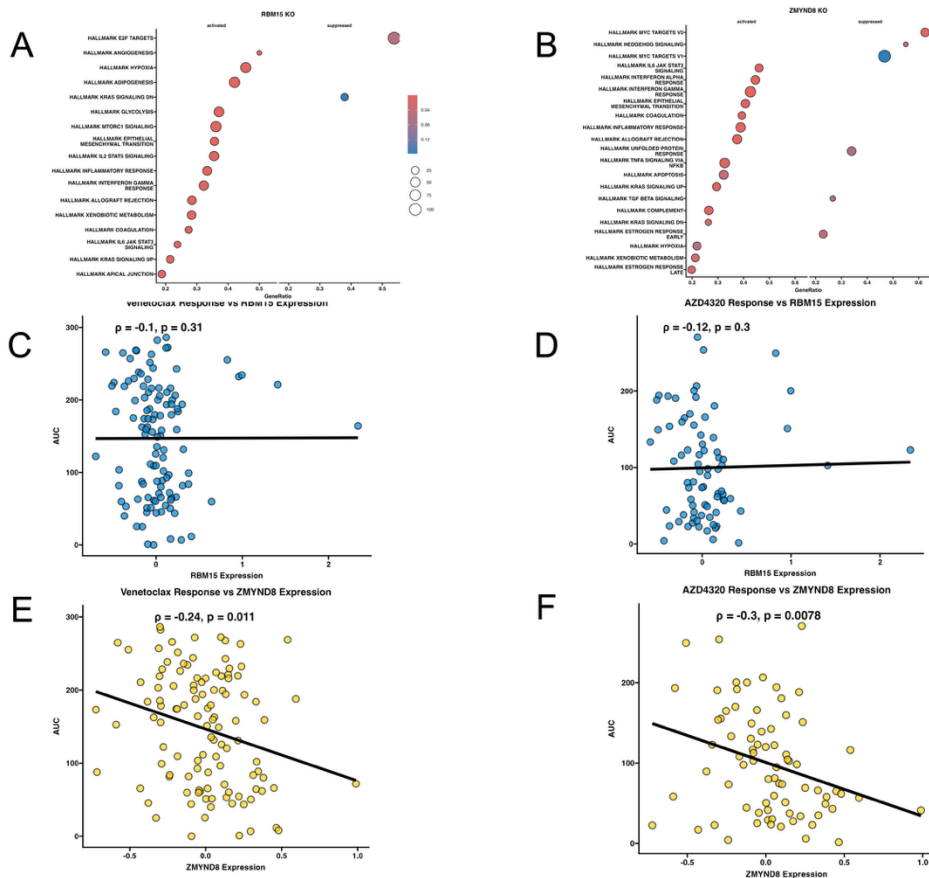


## Supplemental Figures



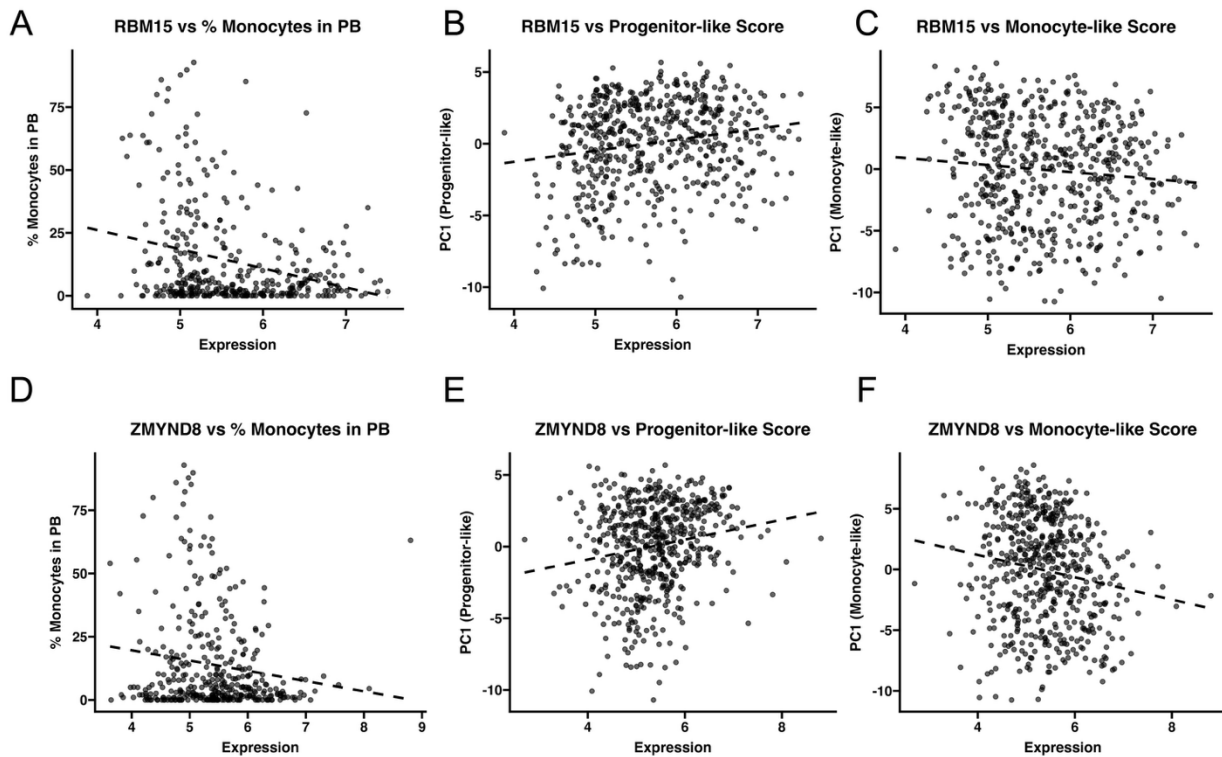
### Supplemental Figure 1: Validation of CRISPR hits from AZD4320 CRISPR Screen.

**(A)** Western blot analysis confirming CRISPR-Cas9-mediated knockout/down of *RBM15* and *ZMYND8*. **(B)** Cell outgrowth assay performed on CRISPR-Cas9 knockout cell lines treated with 30 nM AZD4320, highlighting the drug resistance of *RBM15*-KO and *ZMYND8*-KO cells relative to non-targeting controls (NT). **(C)** Venetoclax sensitivity assay showing the dose-response curves for parental, *RBM15*-KO, and *ZMYND8*-KO cells following a 3-day variable concentration treatment. **(D)** AZD4320 sensitivity assay showing the dose-response curves for parental, *RBM15*-KO, and *ZMYND8*-KO cells following a 3-day variable concentration treatment. **(E)** Response of cell lines to a 3-day inhibitor panel, comparing *RBM15*-KO or *ZMYND8*-KO OCI-AML2 cells (y-axis) to NT control cells (NT, x-axis). Response to venetoclax, AZD4320, or combinations including either are shown in blue.



**Supplemental Figure 2: Investigation of *RBM15* and *ZMYND8* in vivo and in vitro.**

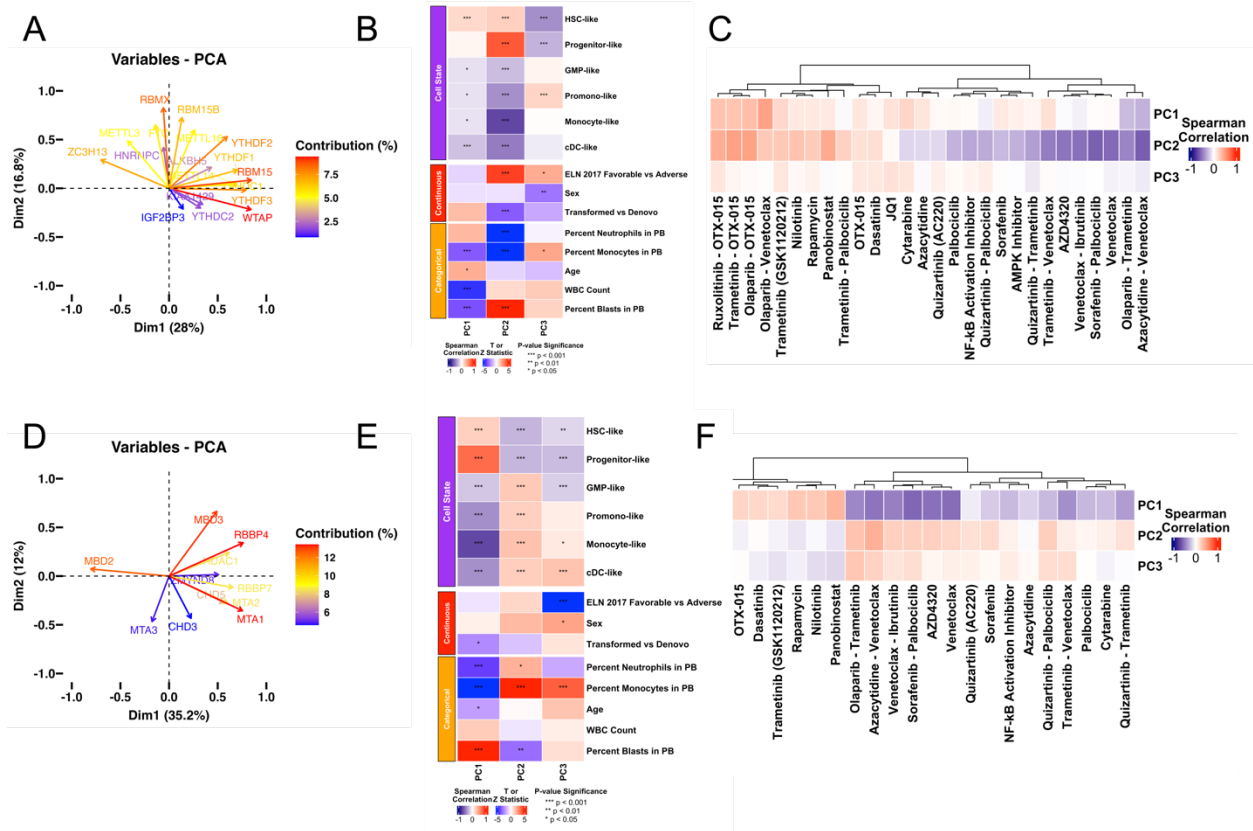
(A) Gene Set Enrichment Analysis (GSEA) using hallmark pathways of differentially expressed genes between *ZMYND8*-KO and NT control cell lines, highlighting significantly enriched Expression pathways. No significant pathway depletion was observed. (B) GSEA using hallmark pathways of differentially expressed genes between *RBM15*-KO and NT control cell lines, highlighting significantly enriched and depleted pathways. (C-F) Correlation between *RBM15* and *ZMYND8* protein expression in patient samples from Beat AML and the AUC values for AZD4320 and venetoclax, respectively.



**Supplemental Figure 3: RBM15 and ZMYND8 RNA expression correlates with differentiation-associated clinical and transcriptional markers.**

(A–C) RBM15 expression plotted against (A) percent monocytes in peripheral blood (PB), (B) progenitor-like score, and (C) monocyte-like score. (D–F) ZMYND8 expression plotted against the same variables: (D) percent monocytes in PB, (E) progenitor-like score, and (F) monocyte-like score.

Percent monocytes in PB is a clinical measurement extracted from electronic medical records from patient from whom samples were obtained, while progenitor-like and monocyte-like scores are transcriptional estimates of differentiation derived from van Galen et al. cell state deconvolution. Linear regression lines are shown for visualization.



### Supplemental Figure 4: m6a and NuRD RNA eigengenes correlate with cell differentiation state and AZD4320 AUC.

**(A)** Principal component analysis (PCA) biplot of m6A pathway gene RNA levels from the Beat AML dataset to generate an m6A eigengene-like signature. **(B)** Correlation of the m6A principal components with cell state scores and clinical differentiation markers, showing negative associations with more differentiated states in principal component 2 (PC2). **(C)** Drug response correlations for the m6A principal components, with PC2 being strongly correlated to resistance to AZD4320 and venetoclax. **(D)** PCA biplot of NuRD complex genes to create a NuRD eigengene-like signature. **(E)** Correlation of the NuRD principal components with cell states and differentiation markers, highlighting associations between PC1 and more differentiated cells. **(F)** Drug response correlations for the NuRD principal components, showing similar resistance patterns with PC1 to AZD4320 and venetoclax.

## Supplemental Tables

<b>m6a Family Gene List</b>	<b>NURD Family Gene List</b>
METTL3	CHD3
METTL14	HDAC1
WTAP	CHD5
RBM15	MBD2
RBM15B	MBD3
METTL16	MTA1
KIAA1429	MTA2
ZC3H13	MTA3
IGF2BP1	RBBP4
IGF2BP3	RBBP7
YTHDC1	ZMYND8
YTHDC2	
YTHDF1	
YTHDF2	
YTHDF3	
HNRNPC	
HNRNPA2BP1	
FTO	
ALKBH5	
RBMX	
IGF2BP2	

### **Supplemental Table 1: Genes included in the m6A and NuRD pathway analyses.**

The m6A pathway gene list was curated through a literature review of known writers, readers, and erasers involved in m6A RNA methylation. The NuRD complex gene list was derived from the HUGO Gene Nomenclature Committee (HGNC) database definition for the NuRD complex gene family. These gene sets were used for principal component analyses and downstream pathway-level correlation analyses presented throughout the manuscript.

Target Gene	Sequence
RBM15_g1_F_1	GAGAGAGCAATTGGCCAATG
RBM15_g1_R_1	CATTGGCCAATTGCTCTCTC
RBM15_g2_F2	CCGATAGCGGCGGTGGGTCG
RBM15_g2_R2	CGACCCACCGCCGCTATCGG
ZMYND8_g1_F1	CTGTTTCAGCTTGGCTGAAG
ZMYND8_g1_R1	CTTCAGCCAAGCTGAAACAG
ZMYND8_g2_F2	CTTACTGAACAGTAACAATA
ZMYND8_g2_R2	TATTGTTACTGTTCAGTAAG

**Supplemental Table 2: Primer sequences used for validation of RBM15 and ZMYND8 knockout cell lines.**

Target	Antibody Product	Vendor	Species	Dilution
RBM15	25261	Cell Signaling	Rb	1:1000
ZMYND8	97845	Cell Signaling	Rb	1:1000
Vinculin	4650	Cell Signaling	Rb	1:1000

**Supplemental Table 3: Antibodies used for Western blotting.**

## Supplemental Data Files (Excel)

### Supplemental Data 1 (CRISPR Screen Results.xlsx):

Genome-wide CRISPR/Cas9 screen results comparing AZD4320-treated versus DMSO-treated OCI-AML2 cells. Contains sgRNA-level counts,  $\log_2$  fold changes, p-values, and gene-level aggregation using the MAGeCK pipeline. Used for identifying genes mediating resistance to AZD4320.

### Supplemental Data 2 (RNA Sequencing Results.xlsx):

Differential expression results from RNA sequencing of RBM15 and ZMYND8 knockout OCI-AML2 cells compared to non-targeting controls. Includes normalized counts,  $\log_2$  fold changes, adjusted p-values (FDR), and gene annotations.

### Supplemental Data 3 (BEAT AML AZD4320 Data.xlsx):

Drug response data from the Beat AML dataset, including AZD4320 area under the curve (AUC) values (derived from a probit regression as in *Bottomly, 2022*). Used in correlation analyses with gene expression and cell state features.

## Supplemental Methods

### Cell Lines and Culture Conditions

Human AML cell line OCI-AML2 was obtained from the ATCC and authenticated using short tandem repeat (STR) profiling at the OHSU DNA Services Core Facility. Cells were maintained in RPMI-1640 medium (Gibco, Thermo Fisher Scientific, Waltham, MA, USA, #11875093) supplemented with 20% fetal bovine serum (FBS; Gibco, #10437028), 2mM L-glutamine (Gibco, #25030081), 100 U/mL penicillin-streptomycin (Gibco, #15140122), and 0.25  $\mu\text{g}/\text{mL}$  amphotericin B (Gibco, #15290018). Cultures were incubated at 37 °C in a humidified atmosphere with 5% CO<sub>2</sub> and passaged every 2–3 days. Mycoplasma contamination was routinely checked.

## Genome-Wide CRISPR/Cas9 Screening

Loss-of-function screens were performed using the Y. Kosuke human genome-wide sgRNA library (Addgene, Watertown, MA, USA, #67989). OCI-AML2 cells expressing Cas9 were generated by transduction with lentivirus carrying the Cas9 construct, followed by selection with blasticidin [10 µg/mL] (InvivoGen, San Diego, CA, USA, #ant-bl-1) for 5-7 days to ensure stable integration. Approximately  $1 \times 10^8$  transduced cells were used to maintain a library coverage of >500 cells per sgRNA.

Cells were transduced with the Y. Kosuke library lentivirus at a multiplicity of infection (MOI) of 0.3 and selected with puromycin (2 µg/mL) for 7 days. Following selection, cells were divided into treatment and control groups. The treatment group was exposed to 30 nM AZD4320 for 14 days, while control cells were treated with an equivalent volume of DMSO (final concentration: 0.1%). Genomic DNA was harvested at days 0, 7, and 14 for downstream analysis.

Genomic DNA was extracted using phenol-chloroform, and sgRNA libraries were amplified using a one-step PCR method to attach Illumina barcodes and primers. Pooled PCR products were sequenced on an Illumina platform. Enriched or depleted sgRNAs were identified by comparing AZD4320-treated and control (DMSO) samples using MAGeCK analysis pipeline described in our previous study.<sup>7</sup> The robust rank aggregation method was applied to compute gene-level p-values, which were adjusted for multiple testing using the Benjamini-Hochberg procedure. Genes with an FDR < 0.05 were considered significant.

CRISPR screen hits were tiered using a method previously described by Nechiporuk et al. (2019). Briefly, sgRNA-level hits were ranked based on three key criteria: effect size ( $\log_2$ -fold change), concordance among guides targeting the same gene, and the number of supporting sgRNAs per gene. A minimum read count of 100 and an FDR < 0.05 were required for inclusion. Tier 1 hits had  $\log_2$ -fold change > 2, >75% of sgRNAs per gene scoring, and >75% concordance among those sgRNAs. Tier 2 hits required  $\log_2$ -fold change > 2 and 100% guide concordance. Tier 3 hits had  $\log_2$ -fold change > 1 and 100% concordance. An additional category of high-confidence

single-guide hits ("singletons") was defined by a  $\log_2$ -fold change  $> 2$ , FDR  $< 0.05$ , and only one targeting guide with  $>100$  reads in the control.

### **Generation and Validation of Knockout Cell Lines**

Lentiviral particles were produced in HEK293T cells by co-transfecting the cells with psPAX2 packaging plasmid (Addgene, #12260), and pMD2.G envelope plasmid (Addgene, #12259) using Lipofectamine 2000 (Invitrogen, #11668019). Viral supernatants were collected at 48- and 72-hours post-transfection, filtered through a  $0.45 \mu\text{m}$  filter, and concentrated by ultracentrifugation at 25,000 rpm for 2 hours at  $4^\circ\text{C}$ .

OCI-AML2 cells were transduced with single guides at an MOI of approximately 0.3 to ensure single integrations per cell. Transduction was performed in the presence of  $8 \mu\text{g/mL}$  Polybrene (Sigma-Aldrich, #TR-1003-G) by spinoculation at  $1,000 \times g$  for 2 hours at  $32^\circ\text{C}$ . Transduced cells were selected with puromycin ( $2 \mu\text{g/mL}$ ) for 7 days to establish stable integration before drug treatment. Knockout efficiency was validated by Western blotting.

Protein lysates were prepared using RIPA buffer supplemented with protease (Roche, #11836170001) and phosphatase inhibitors (ThermoFisher Scientific, #AAJ61022AA). Protein concentrations were determined using the Pierce BCA protein assay (ThermoFisher Scientific, #23227). Samples ( $30 \mu\text{g}$  per lane) were separated by SDS-PAGE on 4-15% polyacrylamide gels (Bio-Rad, Hercules, CA, USA, #4561084) and transferred to PVDF membranes (MilliporeSigma, #IPVH00010). Membranes were blocked with 5% bovine serum albumin (BSA) in Tris-buffered saline with 0.1% Tween-20 (TBST) for 1 hour at room temperature and incubated overnight at  $4^\circ\text{C}$  with primary antibodies. After washing with TBST, membranes were incubated with HRP-conjugated secondary antibodies for 1 hour at room temperature. Bands were visualized using Clarity chemiluminescence (ECL) (Bio-rad, #1705061) substrate and imaged using a ChemiDoc Imaging System (Bio-Rad, #1708280). Antibody details are provided in the supplemental table 3.

## **Cell Proliferation and Viability Assays**

Wild-type (WT), non-targeting control (NT), RBM15 knockout (RBM15 KO), and ZMYND8 knockout (ZMYND8 KO) OCI-AML2 cells were seeded at an initial density of  $2 \times 10^5$  cells/mL in T25 flasks containing 5 mL of complete medium with 30 nM AZD4320 or DMSO. Cells were cultured for 6 days, and viable cell counts were performed every 2 days.

For dose-response assays, cells were seeded in 96-well plates at  $1 \times 10^4$  cells per well in triplicate and treated with serial dilutions of venetoclax or AZD4320 ranging from 0.01 nM to 10  $\mu$ M. After 72 hours of incubation at 37 °C, cell viability was determined by addition of MTS reagent (CellTiter96 AQueous One; Promega Madison, WI, USA) and measurement of absorbance at 490nm. Luminescence was measured using a SpectraMax iD3 microplate reader. Half-maximal inhibitory concentration ( $IC_{50}$ ) values were calculated using nonlinear regression analysis in GraphPad Prism 10 software.

## **RNA Sequencing and Preprocessing**

Total RNA was extracted from OCI-AML2 wild-type, non-targeting control (NT), RBM15 knockout, and ZMYND8 knockout cells using the RNeasy Mini Kit (Qiagen) with on-column DNase digestion to eliminate genomic DNA. RNA quality and quantity were assessed using a NanoDrop spectrophotometer. RNA sequencing libraries were prepared using stranded poly(A)+ selection and sequenced on an Illumina NovaSeq 6000 platform, generating 150 base pair paired-end reads at a target depth of approximately 50 million read pairs per sample.

Paired-end BAM files were aligned to the GRCh38 human reference genome and quantified at the gene level using the featureCounts function with Ensembl gene annotations. Only genes with counts of at least 10 in at least 90% of samples were

retained. Genes with invalid Ensembl IDs or all-zero counts were removed. Ensembl gene identifiers were mapped to HGNC symbols using the org.Hs.eg.db reference database.

Sample condition metadata were extracted from file names and used to classify samples into one of four groups: NT, RBM15, ZMYND8, or parental. Any missing values in the count matrix were set to zero. The resulting filtered count matrix and metadata were used for downstream normalization and differential expression analysis.

### **Differential Expression and Downstream Analysis**

Differential expression analysis was conducted using the DESeq2 framework with negative binomial modeling and dispersion estimation. Surrogate variable analysis (SVA) was performed on the raw count matrix to estimate unmeasured sources of variation. The resulting surrogate variables were incorporated into the design formula for differential testing. Condition labels were set with NT as the reference group.

Differential expression testing was performed for all pairwise comparisons among experimental groups. Genes with an adjusted p-value (Benjamini-Hochberg correction) less than 0.05 were considered statistically significant. No fold-change threshold was applied. Differential expression results, including  $\log_2$  fold change, nominal p-values, and adjusted p-values, were exported for downstream analyses and visualization.

### **Enrichment, Correlation, and Heatmap Analyses**

Gene set enrichment analysis was performed using preranked gene lists based on DESeq2 test statistics. Enrichment was assessed against Hallmark gene sets from the Molecular Signatures Database (MSigDB). Enrichment significance was reported using normalized enrichment scores (NES), nominal p-values, and false discovery rate-adjusted q-values.

Cell type enrichment analysis was conducted using curated lineage-specific marker genes from PanglaoDB. Genes significantly upregulated in knockout conditions were tested for enrichment. Multiple hypothesis correction was applied using the Benjamini-Hochberg method.

For correlation analyses, eigengene-derived scores representing hematopoietic cell states were obtained from previously published methods.<sup>36</sup> These scores were correlated with RBM15 and ZMYND8 expression using Spearman correlation. Statistical significance was calculated using two-sided tests. Heatmaps were generated using normalized expression values or  $\log_2$  fold changes. Genes and samples were clustered using hierarchical clustering with Euclidean distance and complete linkage.

### **m<sup>6</sup>A and NuRD Complex Analyses (Protein and RNA)**

To evaluate the relationship between m<sup>6</sup>A and NuRD complex gene expression and clinical phenotypes, curated gene sets were compiled for each complex. m<sup>6</sup>A family members were selected based on published literature, and NuRD complex components were obtained from the HUGO Gene Nomenclature Committee.

Protein-level expression data were obtained from the PNNL proteomics dataset. RNA-level expression was sourced from the BEAT AML RNA-seq dataset. The resulting principal component scores were merged with BEAT AML clinical annotations, including drug response data (AUC values), cell state scores (vg type and PC1), and other relevant variables. Associations between PCA-derived scores and clinical features were explored using linear regression and correlation, with visualization approaches as described in the relevant figure legends.